Simple all-optical FFT scheme enabling Tbit/s real-time signal processing

D. Hillerkuss[1], M. Winter[1], M. Teschke[1], A. Marculescu[1], J. Li[1], G. Sigurdsson[1], K. Worms[1], S. Ben Ezra[2], N. Narkiss[2], W. Freude[1], and J. Leuthold[1]

[1]*Institute of Photonics and Quantum Electronics, Karlsruhe Institute of Technology (KIT), 76131 Karlsruhe, Germany*
[2]*Finisar Corporation, Nes Ziona, Israel*
[1]*http//:www.ipq.kit.edu*

Abstract: A practical scheme to perform the fast Fourier transform in the optical domain is introduced. Optical real-time FFT signal processing is performed at speeds far beyond the limits of electronic digital processing, and with negligible energy consumption. To illustrate the power of the method we demonstrate an optical 400 Gbit/s OFDM receiver. It performs an optical real-time FFT on the consolidated OFDM data stream, thereby demultiplexing the signal into lower bit rate subcarrier tributaries, which can then be processed electronically.

OCIS codes: (060.4510) Optical communications; (070.2025) Discrete optical signal processing

References and links

1. M. E. Marhic, "Discrete Fourier transforms by single-mode star networks," Opt. Lett. **12**(1), 63–65 (1987).
2. K. B. Howell, *Principles of Fourier Analysis* (CRC Press, 2001).
3. J. W. Cooley, and J. W. Tukey, "An algorithm for the machine calculation of complex Fourier series," Math. Comput. **19**(90), 297–301 (1965).
4. A. E. Siegman, "Fiber Fourier optics," Opt. Lett. **26**(16), 1215–1217 (2001).
5. A. E. Siegman, "Fiber Fourier optics: previous publication," Opt. Lett. **27**(6), 381 (2002).
6. S. Kodama, T. Ito, N. Watanabe, S. Kondo, H. Takeuchi, H. Ito, and T. Ishibashi, "2.3 picoseconds optical gate monolithically integrating photodiode and electroabsorption modulator," Electron. Lett. **37**(19), 1185–1186 (2001).
7. H. Sanjoh, E. Yamada, and Y. Yoshikuni, "Optical orthogonal frequency division multiplexing using frequency/time domain filtering for high spectral efficiency up to 1 bit/s/Hz," in *Proceedings of Optical Fiber Communication Conference and Exhibit,* (Optical Society of America, 2002), paper ThD1.
8. C. K. Madsen, and J. H. Zhao, *Optical Filter Design and Analysis: A Signal Processing Approach* (Wiley-Interscience, 1999).
9. B. H. Verbeek, C. H. Henry, N. A. Olsson, K. J. Orlowsky, R. F. Kazarinov, and B. H. Johnson, "Integrated four-channel Mach-Zehnder multi/demultiplexer fabricated with phosphorous doped SiO_2 waveguides on Si," J. Lightwave Technol. **6**(6), 1011–1015 (1988).
10. N. Takato, K. Jinguji, M. Yasu, H. Toba, and M. Kawachi, "Silica-based single-mode waveguides on silicon and their application to guided-wave optical interferometers," J. Lightwave Technol. **6**(6), 1003–1010 (1988).
11. S. Suzuki, Y. Inoue, and T. Kominato, "High-density integrated 1×16 optical FDM multi/demultiplexer," in *Proceedings of Lasers and Electro-Optics Society Annual Meeting* (IEEE, 1994), pp. 263–264.
12. N. Takato, T. Kominato, A. Sugita, K. Jinguji, H. Toba, and M. Kawachi, "Silica-based integrated optic Mach-Zehnder multi/demultiplexer family with channel spacing of 0.01-250 nm,"," IEEE J. Sel. Areas Comm. **8**(6), 1120–1127 (1990).
13. K. Takiguchi, M. Oguma, T. Shibata, and H. Takahashi, "Demultiplexer for optical orthogonal frequency-division multiplexing using an optical fast-Fourier-transform circuit," Opt. Lett. **34**(12), 1828–1830 (2009).
14. A. J. Lowery, L. B. Du, and J. Armstrong, "Performance of optical OFDM in ultralong-haul WDM lightwave systems," J. Lightwave Technol. **25**(1), 131–138 (2007).
15. A. Lowery, and J. Armstrong, "Orthogonal-frequency-division multiplexing for dispersion compensation of long-haul optical systems," Opt. Express **14**(6), 2079–2084 (2006).
16. W. Shieh, and I. Djordjevic, *OFDM for Optical Communications* (Academic Press, 2010).
17. J. Armstrong, "OFDM for optical communications," J. Lightwave Technol. **27**(3), 189–204 (2009).
18. R. P. Giddings, X. Q. Jin, and J. M. Tang, "First experimental demonstration of 6Gb/s real-time optical OFDM transceivers incorporating channel estimation and variable power loading," Opt. Express **17**(22), 19727–19738 (2009).

#124508 - $15.00 USD Received 19 Feb 2010; revised 2 Apr 2010; accepted 15 Apr 2010; published 20 Apr 2010

19. Q. Yang, S. Chen, Y. Ma, and W. Shieh, "Real-time reception of multi-gigabit coherent optical OFDM signals," Opt. Express **17**(10), 7985–7992 (2009).
20. Y. Benlachtar, P. M. Watts, R. Bouziane, P. Milder, D. Rangaraj, A. Cartolano, R. Koutsoyannis, J. C. Hoe, M. Püschel, M. Glick, and R. I. Killey, "Generation of optical OFDM signals using 21.4 GS/s real time digital signal processing," Opt. Express **17**(20), 17658–17668 (2009).
21. H. C. Hansen Mulvad, M. Galili, L. K. Oxenløwe, H. Hu, A. T. Clausen, J. B. Jensen, C. Peucheret, and P. Jeppesen, "Demonstration of 5.1 Tbit/s data capacity on a single-wavelength channel," Opt. Express **18**(2), 1438–1443 (2010).
22. E. Yamada, A. Sano, H. Masuda, T. Kobayashi, E. Yoshida, Y. Miyamoto, Y. Hibino, K. Ishihara, Y. Takatori, K. Okada, K. Hagimoto, T. Yamada, and H. Yamazaki, "Novel no-guard-interval PDM CO-OFDM transmission in 4.1 Tb/s (50 × 88.8-Gb/s) DWDM link over 800 km SMF including 50-Ghz spaced ROADM nodes," in *Proceedings of Optical Fiber Communication Conference and Exposition and The National Fiber Optic Engineers Conference* (Optical Society of America, 2008), paper PDP8.
23. S. Chandrasekhar, X. Liu, B. Zhu, and D. W. Peckham, "Transmission of a 1.2-Tb/s 24-carrier no-guard-interval coherent OFDM superchannel over 7200-km of ultra-large-area fiber," in *Proceedings of European Conference on Optical Communication* (IEEE, 2009), paper PD2.6.
24. A. D. Ellis, and F. C. G. Gunning, "Spectral density enhancement using coherent WDM," IEEE Photon. Technol. Lett. **17**(2), 504–506 (2005).
25. Y. Ma, Q. Yang, Y. Tang, S. Chen, and W. Shieh, "1-Tb/s single-channel coherent optical OFDM transmission over 600-km SSMF fiber with subwavelength bandwidth access," Opt. Express **17**(11), 9421–9427 (2009).
26. W. Shieh, H. Bao, and Y. Tang, "Coherent optical OFDM: theory and design," Opt. Express **16**(2), 841–859 (2008).
27. T. Kobayashi, A. Sano, E. Yamada, Y. Miyamoto, H. Takara, and A. Takada, "Electro-optically multiplexed 110 Gbit/s optical OFDM signal transmission over 80 km SMF without dispersion compensation," Electron. Lett. **44**(3), 225–226 (2008).
28. D. Hillerkuss, A. Marculescu, J. Li, M. Teschke, G. Sigurdsson, K. Worms, S. Ben Ezra, N. Narkiss, W. Freude, and J. Leuthold, "Novel optical fast Fourier transform scheme enabling real-time OFDM processing at 392 Gbit/s and beyond," in *Proceedings of Optical Fiber Communication Conference and Exposition and The National Fiber Optic Engineers Conference* (Optical Society of America, 2010), paper OWW3.

1 Introduction

The fast Fourier transform (FFT) is a universal mathematical tool for almost any technical field. In practice it either relates space and spatial frequencies (spatial FFT) or time and temporal frequency (temporal FFT). While the former can most easily be implemented in the optical domain by means of a lens, the time-to-frequency conversion in the optical domain is more intricate. Yet, it is exactly this conversion that is needed for next generation signal processing such as required for OFDM in optical communications. The importance of the optical FFT for the implementation of next generation processors has been recognized in the past, and direct implementations of the FFT in integrated optics technology have been suggested by Marhic et al. [1] and others. However, to this point these schemes are difficult to implement and stabilize, and they do not scale well with increasing FFT order.

In this paper, we introduce a new and practical implementation of the optical FFT. We discuss the feasibility, tolerances towards further simplifications, practical implementations, and we demonstrate the potential of the method by an exemplary implementation for a next generation OFDM system. We show that a single 400 Gbit/s OFDM channel can be demultiplexed into its constituting subchannels by optical means. The method is based on passive optical components only and thus basically provides processing without any power consumption. The scheme therefore is in support of a new paradigm, where all-optical and electronic processing synergistically interact providing their respective strengths. All-optical methods allow processing at highest speed with little – if no power consumption, and electronic processing performs the fine granular processing at medium to low bit rates.

In Section 2 we introduce the new optical FFT. In Section 3 we show how the optical FFT and IFFT can be applied to OFDM transmission systems in order to enable processing of OFDM-channels at very high bit rates without the limitations of the electronic circuits. In Section 4, we will present the results of an experimental implementation of the optical FFT for demultiplexing a consolidated OFDM signal into its OFDM subchannels.

#124508 - $15.00 USD Received 19 Feb 2010; revised 2 Apr 2010; accepted 15 Apr 2010; published 20 Apr 2010

2 The optical FFT/IFFT

In this section we introduce the new optical FFT method. We first recapitulate conventional means for performing the optical FFT and differentiate it from the commonplace FFT as done with a computer. We then show how subtle re-ordering of the various FFT circuit elements leads to a significant reduction of the complexity. It also leads to a simple and practical optical circuit with an equivalent output. Afterwards we show how this circuit can be further simplified at the cost of a small interchannel crosstalk penalty by replacing one or more stages of the FFT circuit by standard optical (tunable) filters.

2.1 Background

The fast Fourier transform (FFT) is an efficient method to calculate the discrete Fourier transform (DFT) for a number of time samples N, where $N = 2^p$ with p being an integer. The N-point DFT is given as

$$X_m = \sum_{n=0}^{N-1} \exp\left[-\mathrm{j}2\pi \frac{mn}{N}\right] x_n \quad , \quad m = 0,..,N-1 \tag{1}$$

transforming the N inputs x_n into N outputs X_m. If the x_n represent a time-series of equidistant signal samples of signal $x(t)$ over a time period T, as shown in Fig. 1(a), then the X_m will be the unique complex spectral components of signal x repeated with period T [2]. The FFT typically "decimates" a DFT of size N into two interleaved DFTs of size $N/2$ in a number of recursive stages [3] so that

$$X_m = \begin{cases} E_m + \exp\left[-\mathrm{j}\dfrac{2\pi}{N}m\right] O_m & \text{if } m < \dfrac{N}{2} \\ E_{m-N/2} - \exp\left[-\mathrm{j}\dfrac{2\pi}{N}\left(m - \dfrac{N}{2}\right)\right] O_{m-N/2} & \text{if } m \geq \dfrac{N}{2} \end{cases} \tag{2}$$

The quantities E_m and O_m are the *e*ven and *o*dd DFT of size $N/2$ for even and odd inputs x_{2l} and x_{2l+1} ($l = 0,1,2,\ldots N/2-1$), respectively. Figure 1(b) shows the direct implementation of the FFT for $N = 4$ using time electrical sampling and signal processing. Marhic [1] and Siegman [4,5] have shown independently a possible implementation of an optical circuit which performs an FFT. Such an implementation for $N = 4$ is shown in Fig. 1(c). When using an optical circuit to calculate the FFT the outputs X_m appear instantaneously for any given input combination x_n. Thus, in order to obtain the spectral components of a time series, the N time samples in interval T must be fed simultaneously into the circuit. This can be achieved using optical time delays as a serial-to-parallel (S/P) converter, as shown in Fig. 1(c).

The optical FFT (OFFT) differs from its electronic counterpart by its continuous mode of operation. In an electronic implementation optimized for highest throughput, the optical signal is sampled and the FFT is computed from all samples x_n. Afterwards, the next N samples are taken. In the optical domain, the FFT is computed continuously. Yet, the calculation is correct only when feeder lines 1 to N contain the time samples from within their respective interval. Sampling must therefore be performed in synchronization with the symbol over a duration of T/N. These samples subsequently can be processed in the optical FFT stage. However, it must be emphasized that proper calculation is only possible if all samples are forwarded from one stage to the next stage in synchronism. Care must therefore be taken, that not only all waveguides interconnecting the couplers have equal delay but also maintain proper phase relations, as indicated in optical FFT stage of Fig. 1(c).

#124508 - $15.00 USD Received 19 Feb 2010; revised 2 Apr 2010; accepted 15 Apr 2010; published 20 Apr 2010

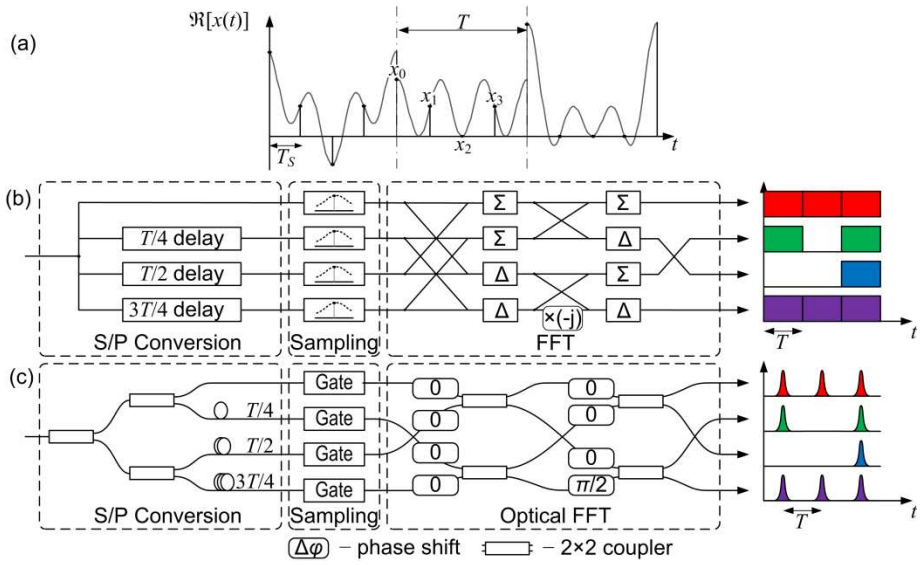

Fig. 1. Four point example of the traditional fast Fourier transform and its optical equivalent. (a) Exemplary signal in time sampled at $N = 4$ points; (b) the structure consists of a serial-to-parallel (S/P) conversion that generates parallel samples of the signal, a sampling stage to generate the time samples x_n and a conventional FFT stage that calculates the fast Fourier transform of the sampled signal; (c) the optical equivalent of the circuit uses passive splitters and optical time delays for serial-to-parallel conversion; optical gates perform the sampling of the optical waveform; afterwards the optical FFT is computed using optical 2 × 2 couplers and phase shifts as described in [1]. Right-hand sides of (b) and (c) show typical output signals for input signal (a).

The optical FFT has several advantages over its electronic counterpart. First, the all-optical FFT may be used at highest speeds where electronics cannot be used. This is due to the fact that the optical sampling window sizes (e. g., with electro-absorption modulators, EAM) can be significantly shorter than electronic sampling windows of analog-to-digital converters (ADC) [6]. Additionally, since all components used in the OFFT are passive (except for tuning circuitry and time gating), the power consumption is inherently low and barely increases with complexity or sampling rate. For an exemplary 8-point FFT of a 28 GBd OFDM signal, we estimate the power consumption for the optical and the electrical sampling as follows. The power requirement for the optical sampling of 8 tributaries is dominated by the EAM driver amplifiers and would be about 14 W. In addition, several watts will be required to compensate for insertion and modulation loss of the optical gates using optical amplifiers. In comparison to this, the power consumption for electrical sampling at the required sampling rate of 224 GSa/s for I and Q is estimated to be in excess of 160 W. This power value is calculated by interpolation from state of the art analog-to-digital converters (ADCs). A state of the art ADC at 28 GSa/s consumes at least 10 W of electrical power. If higher sampling rates are implemented using parallelization, the power consumption increases linearly. If no guard interval is used, a sampling rate of 224 GSa/s on two ADCs is required leading to the estimated total power of 160 W. Introducing a guard interval at the same overall bitrate would increase the power consumption of the electronic implementation as digitizing of the guard interval is also needed. In comparison to this, the power consumption of the optical implementation will not increase, as the number of required optical gates does not change with the introduction of a guard interval. It has to be pointed out, that the power consumption for the electronic sampling also includes the analog-to-digital conversion.

A disadvantage of this approach is the unfortunate scaling with size. The number of couplers is the complexity $C_{\text{std}} = N - 1 + (N/2)\log_2 N$, and the optical phases in all $N\log_2(N)$ arms

#124508 - $15.00 USD Received 19 Feb 2010; revised 2 Apr 2010; accepted 15 Apr 2010; published 20 Apr 2010

of the FFT structure must be stabilized with respect to each other, thereby limiting N to a small number for practical cases. This renders the optical approach according to Fig. 1(c) impractical for large N. Electronic signal processing that could be used instead is, however strongly limited due to its power consumption and its limited speed. However, it is possible to significantly simplify the circuit of Fig. 1(c) without affecting its operation.

It has to be mentioned that another possible scheme uses waveguide grating routers (WGR) to implement the DFT [7]. This approach, however, suffers from the need to control the relative phases of all N paths of the structure simultaneously, requiring N-1 Phase shifters.

2.2 A new optical FFT scheme

Here we show that by re-ordering the delays and by re-labeling the outputs accordingly an equivalent but simpler implementation can be found, since a direct implementation of the circuit in Fig. 1(c) would be difficult to make due to its frequent waveguide crossings, and due to the large number of waveguide phases that need to be accurately controlled.

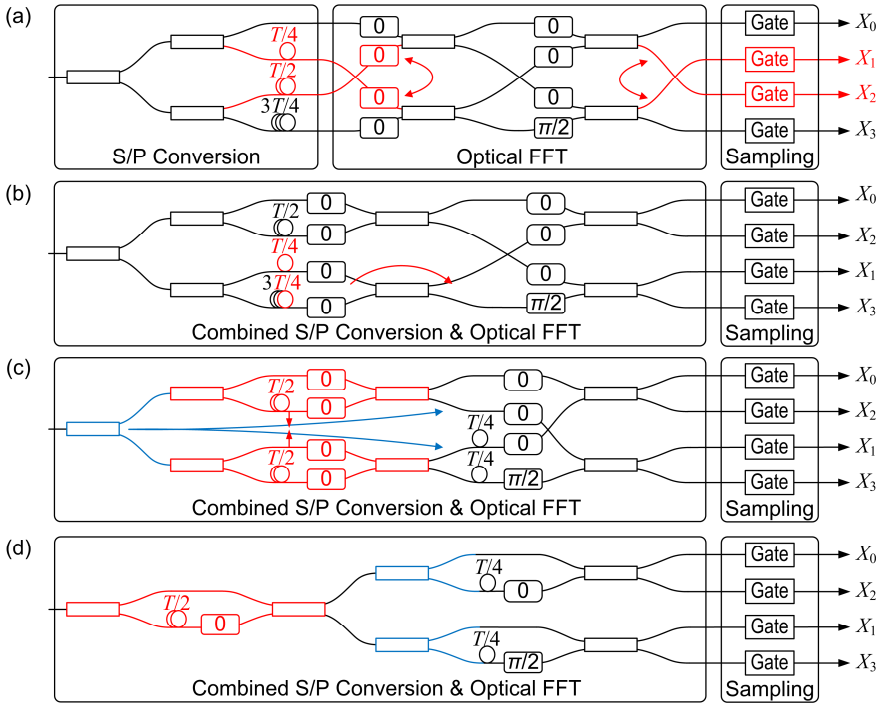

Fig. 2. Exemplary four-point optical FFT for symbol period T; (a) traditional implementation as in Fig. 1; (b) leading to a structure consisting of two DIs with the same differential delay; the additional $T/4$ delay is moved out of the second DI (c), which leads to two identical DIs that can be replaced by a single DI followed by signal splitters; (d) low-complexity scheme with combined S/P conversion and FFT.

The simplifying steps for an example with $N = 4$ are shown in Fig. 2. In a first step we re-locate the sampling gates to the end of the circuit. This will not change the overall operation. Next we re-order the delays in the S/P conversion stage as indicated in Fig. 2(a) and re-label the outputs accordingly. This way the OFFT input stage consists of two parallel delay interferometers (DIs) with the same free spectral range (FSR) but different absolute delays (cf. Figure 2(b)). By moving the common delay of $T/4$ in both arms of the lower DI to its outputs, one obtains two identical DIs with the same input signal, see Fig. 2(c). This redundancy can be eliminated by replacing the two DIs with one DI and by splitting the output. The process is illustrated in Fig. 2(d). These simplification rules can be iterated to apply to FFTs of any size

#124508 - $15.00 USD Received 19 Feb 2010; revised 2 Apr 2010; accepted 15 Apr 2010; published 20 Apr 2010

N. The new optical FFT processor consists only of $N-1$ cascaded DIs with a small complexity of only $C_{\mathrm{DI}} = 2(N-1)$ couplers, where $C_{\mathrm{DI}} \le C_{\mathrm{std}}\ \forall N$. Also, in this implementation only the phase of $N-1$ DIs needs stabilization, and no inter-DI phase adjustment is required.

In the Appendix it is shown mathematically that the DFT of order $N = 2^p$ as described by Eq. (1) can always be replaced by an arrangement of p DI stages as indicated in Fig. 2(d). The DI delay in each stage and the location of the necessary phase shifters are derived as well. For illustration we show the structure for $N = 8$ in Fig. 3(a) as derived with the optical FFT approach according to [1] and in Fig. 3(b) the new structure presented in this contribution.

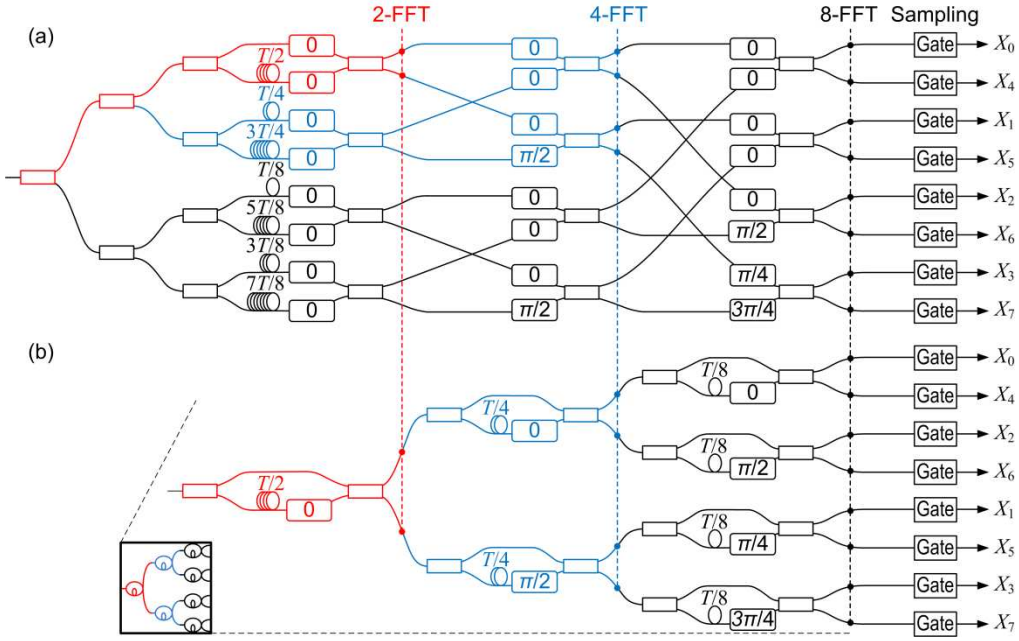

Fig. 3. (a) Direct FFT implementation versus (b) simplified all-optical FFT circuit for $N = 8$ showing the arrangement of delays and phase shifts as derived in Appendix A. The order of the outputs is different from that of the conventional FFT scheme. The sub-circuits for the FFT of order 2 and 4 are also marked, respectively.

An inherent advantage of this approach is that a single frequency component of the sampled signal can be easily extracted without the implementation of the complete structure. In this case all DIs that are not part of the optical path to the corresponding output port can be removed, leaving only one DI per stage and thus a total of $\log_2 N$ DIs that require stabilization. By tuning the phases in each DI, any arbitrary FFT coefficient of the signal can be selected without changing the structure of the setup, as illustrated in Fig. 4. Such a reduction in complexity is not possible with the structures that have been shown previously (see Section 2.1). The ability to shape the spectral (Fourier) components of an optical signal with a structure similar to that in Fig. 4 makes it a member of the family of *Fourier filters* [8]. However, in order to obtain the block-wise DFT of an optical signal, a Fourier filter is not sufficient. Instead, the complete structure according to Fig. 3 is required, including the time-domain optical sampling which is an essential part of the DFT or short-time Fourier Transform (STFT), as we will show.

#124508 - $15.00 USD Received 19 Feb 2010; revised 2 Apr 2010; accepted 15 Apr 2010; published 20 Apr 2010

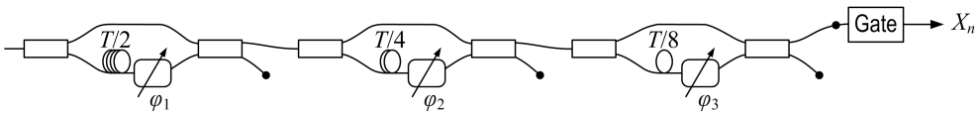

Fig. 4. Optical FFT circuit based on Fig. 3 for the extraction of Fourier component X_n. By tuning the phases φ_1, φ_2 and φ_3, any required Fourier component may be extracted without physically changing the setup.

The frequency response of the DI cascade can be easily visualized, cf. Figure 5. As a matter of fact, the DFT of order N is able to discriminate N individual frequency components of the input signal, spaced $\Delta\omega = 2\pi/T_S$ apart, as theoretically shown in the Appendix. Thus, by cascading a sufficient number of DIs with correct delay and phase, any arbitrary frequency component can be isolated. Figure 5 shows that switching between outputs X_0 and X_4 can be achieved by simply tuning $\varphi_3 = 0$ to $\varphi_3 = \pi$, thus shifting the green curve, equivalent to using the second (lower) output of the DI.

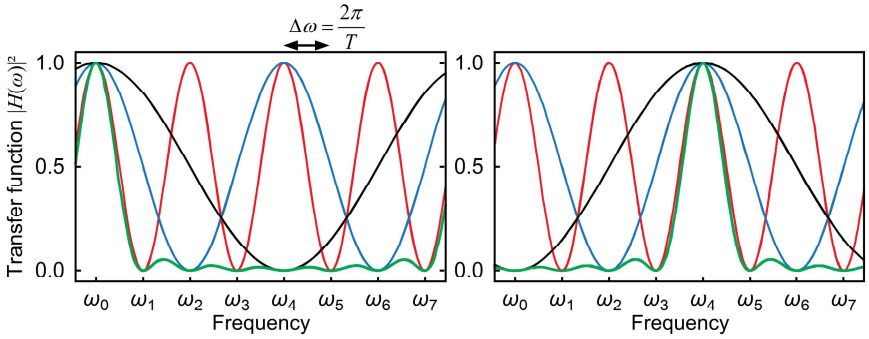

Fig. 5. Exemplary illustration of the intensity transfer functions of each stage (blue, red, and green) in the cascade of Fig. 3 and the total transfer function of the FFT circuit (black) for outputs X_0 (left side) and X_4 (right side).

The cascade of DIs has previously been proposed as a demultiplexer for FDM channels that do not overlap, functioning as a filter bank [7,9–12]. Its adaptation to OFDM, which is based on the STFT/FFT property of the structure, however, is only possible in combination with optical sampling to delineate the OFDM symbol boundaries.

The traditional optical FFT according to Marhic [1] supplemented by optical sampling has also been implemented as OFDM demultiplexer by Takiguchi et al. [13] for $N = 4$. However, due to the complexity of the approach it does not scale well for larger N.

2.3 A further simplification

Figure 5 has shown that the DFT acts as a periodic filter in the frequency domain with a FSR of $N\Delta\omega$, and each DI of the cascade is also a periodic filter with FSR $N\Delta\omega/2^p$ where p is the index of the FFT stage and N is the order of the FFT. In order to further simplify the optical FFT circuit, one might be tempted to replace one or more stages of the DI cascade by standard (non-DI) optical filters. Since the stages with a higher subscript (those being traversed last) have the largest FSR, it would be sensible to replace these first, because the requirements on these filters are most relaxed. In Fig. 6 we have reduced the number of DI stages of an $N = 8$ FFT from top to bottom and replaced them by a single Gaussian filter (for illustration purposes).

#124508 - $15.00 USD Received 19 Feb 2010; revised 2 Apr 2010; accepted 15 Apr 2010; published 20 Apr 2010

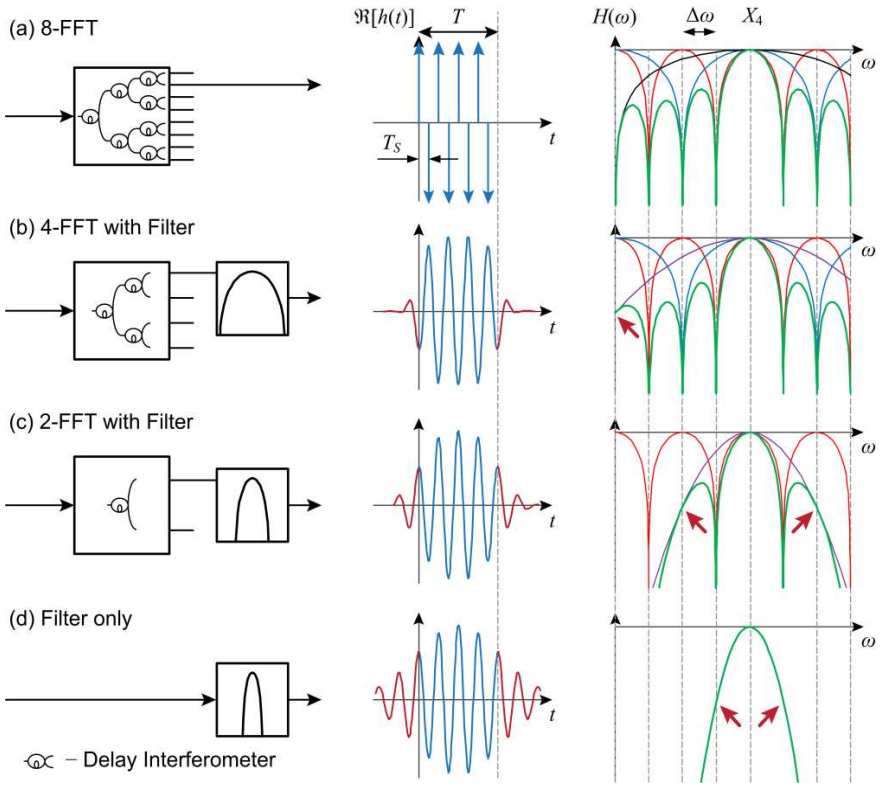

Fig. 6. Inter-symbol interference and frequency crosstalk occurring when replacing (parts of) the DI filters by 1st-order Gaussian filters with appropriate passbands in order to extract frequency component X_4. The left column shows the setup schematic, the middle column shows the real part of the impulse response and the right column shows the logarithmic intensity transfer functions of the involved DI stages (blue, red, and green), the optical filter (purple) and their cascade (black). In case of the approximations, the transfer function is not nulled for all outputs except X_4, leading to frequency crosstalk (red arrows). Also with decreasing filter bandwidth, the impulse response exceeds the DFT summation interval T (marked red), leading to crosstalk/interference from neighboring time slots.

Figure 6(a) shows the original optical FFT with $N = 8$ together with the impulse response of output X_2. With the derivation given in Eq. (10) of the Appendix the impulse response at output X_2 is

$$h_4(t) = \frac{1}{8}\left[\sum_{n=0}^{3}\delta\left(t-\frac{2n+1}{8}T\right)-\sum_{k=0}^{3}\delta\left(t-\frac{2n}{8}T\right)\right] \tag{3}$$

and the corresponding frequency transfer function is

$$H_4(\omega) = \frac{1}{8}\left[1+\exp\left(-\mathrm{j}\left[\omega\frac{T}{2}\right]\right)\right]\left[1+\exp\left(-\mathrm{j}\left[\omega\frac{T}{4}\right]\right)\right]\left[1+\exp\left(-\mathrm{j}\left[\omega\frac{T}{8}+\pi\right]\right)\right] \tag{4}$$

If the third OFFT stage is replaced by a Gaussian filter (bank) as in Fig. 6(b), the FFT order is reduced to $N = 4$, which reduces the OFFT to two DI stages only. The impulse response then is described by the convolution of the response of the first two stages, which consists of 4 impulses according to Eq. (10) given in the Appendix, with the impulse response of a 1st-order Gaussian filter centered at ω_F,

#124508 - $15.00 USD Received 19 Feb 2010; revised 2 Apr 2010; accepted 15 Apr 2010; published 20 Apr 2010

$$h_{\text{Gauss}}(t) = \frac{1}{\sqrt{2\pi}\cdot\delta}\exp\left(-\frac{t^2}{2\delta^2}\right)\exp\left(-\mathrm{j}\omega_F t\right) \quad \text{with} \quad \delta = \frac{\sqrt{\ln 2}}{\omega_B T} \tag{5}$$

where ω_B is the 3 dB bandwidth of the filter. As can be seen in the frequency response in Fig. 6(b), this replacement causes crosstalk from frequency component X_0 (red arrow). Furthermore, due to the significantly longer impulse response of the Gaussian filter, the total filter impulse response is increased (marked red) and causes inter-symbol interference (ISI). If more DI stages are replaced by optical filters, the filter passband in the frequency domain must become narrower. By the Fourier uncertainty principle [2] this results in an even longer impulse response and thus larger ISI, as shown in Figs. 6(c) and 6(d).

2.4 Implementation

The all-optical (I)FFT structure presented in the previous section can be implemented straightforwardly using free-space optics or integrated optical circuits. Previously, implementations of DI cascades for up to $N = 16$ have been shown using the silica-on-silicon approach [9–12]. Integration in material systems of more recent interest such as silicon-on-insulator or InP is expected to yield much more compact structures, but has to our knowledge not yet been published. Benefits of optical integration are the small footprint and ease of stabilization.

3 Application to orthogonal frequency-division multiplexing (OFDM)

OFDM is a multicarrier signaling technique that has emerged as a promising technology for ultra-high bit rate transmission. The reason lies in its potentially high spectral efficiency, which can be significantly higher than wavelength-division multiplexing (WDM), and its tolerance to transmission impairments like dispersion [14,15]. A detailed overview of the state-of-the-art concerning OFDM transmission is available in [16].

In OFDM, the tributaries or subcarriers are spaced so tightly that their spectra overlap, whereas in WDM they are separated by guard bands which enable channel extraction by means of conventional optical filters, as shown in Fig. 7. The whole of the subcarriers in an OFDM channel form a signal in time – the OFDM signal, which can no longer be demodulated by a simple filter due to the spectral overlap of its tributaries. Its shape in time is an analog signal as was illustrated in Fig. 1. Yet if the subcarrier frequency spacing $\Delta\omega$ is related to the duration T by

$$\Delta\omega = \frac{2\pi}{T} \tag{6}$$

then two subcarriers p and q are orthogonal with respect to integration over an interval T,

$$\frac{1}{N}\sum_{n=0}^{N-1}\exp\left[\mathrm{j}\,p\Delta\omega\frac{nT}{N}\right]\exp\left[\mathrm{j}\,q\Delta\omega\frac{nT}{N}\right] = \begin{cases}1 & \text{if } p = q\\ 0 & \text{else}\end{cases} \tag{7}$$

As a consequence, an appropriate receiver will be able to distinguish them. Such receivers exist. They almost exclusively perform the FFT/STFT on the time-sampled signal in the electronic domain [17]. Such electronic real-time implementations are currently restricted to OFDM symbol rates of a few MBd due to speed limitations of the digital signal processor [18,19]. These symbol rates correspond to total bitrates of several Gb/s as a large number of subcarriers and higher order modulation formats are used. Higher bit rate OFDM signals usually have to be processed offline, which may be practicable for laboratory experiments but not for data transmission [20].

In this section we propose our low-complexity scheme based on the optical FFT, in which the demultiplexing of the OFDM subchannel is performed in the optical domain, and only the subchannel signal processing is done in the electronic domain. This way it is only the subchannel symbol rate that is limited by the capabilities of the electronic receiver.

#124508 - $15.00 USD Received 19 Feb 2010; revised 2 Apr 2010; accepted 15 Apr 2010; published 20 Apr 2010

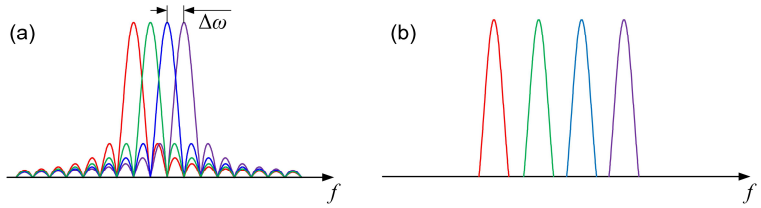

Fig. 7. Optical spectra of (a) an OFDM signal with 4 subchannels and (b) a DWDM signal with 4 channels. Due to the overlap, the OFDM subchannels cannot be extracted by simple optical filtering and the whole of the spectrum has to be processed simultaneously.

Two possible implementations exploiting the OFFT are depicted in Fig. 8. In Fig. 8(a), the optical inverse FFT (IFFT) is used to generate the OFDM signal and the optical FFT is used for demultiplexing. Here, the pulse train at rate T^{-1} from the mode-locked laser (MLL) is split and modulated independently with an arbitrary subcarrier modulation format for each subcarrier. The modulated pulse trains are subsequently fed into the optical IFFT circuit, which transforms them into an OFDM signal that consists of individual pulses of a length of ~T_S, not unlike an OTDM signal [21]. Each of the output pulses of the optical FFT is a superposition of copies of the different input pulses with different phase coefficients. The spectrum of the generated signal is significantly wider than expected for an OFDM signal. To obtain the same waveform and spectrum as in the second approach, it is necessary to limit the bandwidth of the signal using bandpass filtering of the output signal or pulse shaping of the MLL. The main difference to an OTDM signal, which consists of a series of pulses of (ideally) equal amplitude, is that each pulse is a superposition of N subchannel samples with a corresponding variation in pulse amplitude, and the combination of N such pulses forms a single OFDM symbol. This transmitter is described in detail in Section 3.1. In Fig. 8(b), a frequency comb, here provided by a MLL is split into its (non-overlapping) Fourier components by a waveguide grating router (WGR). The Fourier components of the input signals are directly modulated at a symbol rate chosen such that condition (7) is fulfilled. The tributaries, or subchannels, are then recombined to obtain the OFDM signal. This transmitter is described in detail in Section 3.2.

In both cases, the receiver part consists of the optical FFT to demultiplex the OFDM signal into its tributaries and a subcarrier receiver "subchannel Rx". The exact details of the subcarrier Rx in Fig. 8 varies with the modulation format used within the subchannels. It could be a direct detection receiver, a balanced DI receiver such as needed for DPSK signals, a DQPSK receiver, or a coherent receiver for QPSK or any other QAM signal.

Comparing OFDM and OTDM at similar bitrates, one can observe some similarities, but also significant differences. Probably the most important ones can be found in the resilience with respect to chromatic dispersion. In OFDM systems, the dispersion tolerance can be tuned by a proper choice of subchannel bandwidth, and by the insertion of a cyclic prefix. As we have shown in Section 2.3, the extraction of an OFDM subband before demultiplexing can further increase the dispersion tolerance. On the other hand, OTDM requires that narrow symbols remain narrow, and thus requires higher-order dispersion compensation in order to be properly demultiplexed [21]. Also, it is not possible to access a fraction of the OTDM signal using optical filtering, as it can be done for the in the subband access in OFDM signals. Lastly, OFDM requires the various lines of the comb source spectrum to be locked relative to each other only in frequency, whereas for OTDM (and the IOFFT transmitter of Section 3.1) the spectral lines need to obey strict phase relations in order to obtain sufficiently short pulses.

#124508 - $15.00 USD Received 19 Feb 2010; revised 2 Apr 2010; accepted 15 Apr 2010; published 20 Apr 2010

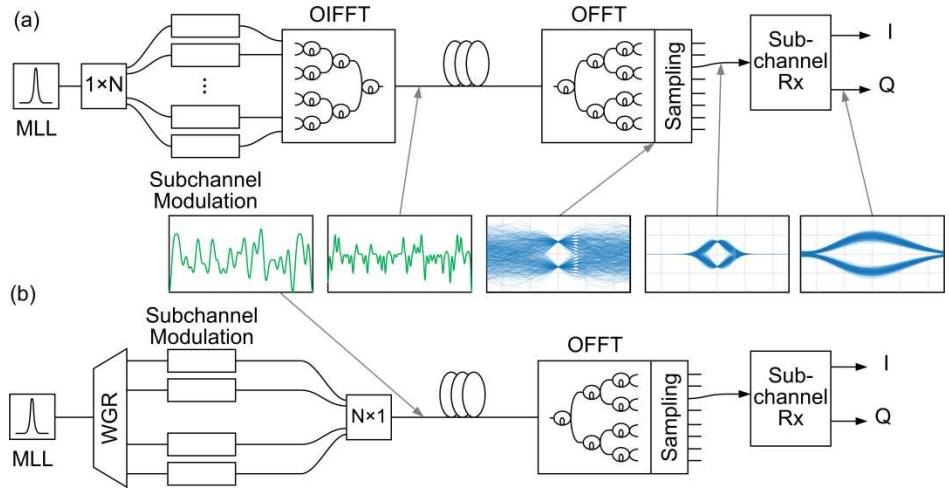

Fig. 8. Two examples for the implementation of an all-optical OFDM transmitter-receiver pair. (a) The output of a pulse source (e.g. a mode-locked laser) is split onto *N* copies and each copy of the pulse train is encoded individually with an arbitrary subcarrier modulation format before being combined in the optical IFFT circuit. (b) The output of a pulse or frequency comb source is split into its spectral components, each of which satisfies Eq. (7). Those spectral components are separately encoded with an arbitrary subcarrier modulation format and combined to form the OFDM signal. At the receiver, the subchannels are separated using the optical FFT circuit. The receiver is identical to the one above. Green insets show exemplary waveforms before WDM filtering at the transmitter with OTDM-like pulses after the optical IFFT. Blue insets show exemplary eye diagrams at various locations within the receiver.

3.1 OFDM using the optical IFFT

The optical FFT can be used for both, the implementation of the transmitter and of the receiver, Fig. 8(b). At the transmitter, the IFFT creates the OFDM symbols with the configuration of Fig. 3, whereas the signals would traverse the structure in the inverse direction, coming from the right. A short pulse launched into any of the IFFT circuit inputs will result in a series of pulses with equal shapes but correspondingly lower pulse energy to appear at the output of the circuit. In order for these pulses not to interfere with one another or with pulses from neighboring OFDM symbols, the duration of these input pulses must be sufficiently short (on the order of *T*/*N*). The input pulses can then be encoded with an arbitrary modulation format (e.g. QPSK or QAM) prior to injection into the optical IFFT circuit to obtain a sequence of OFDM symbols. At the receiver, the optical FFT circuit demultiplexes the OFDM symbols continuously. Correct outputs are obtained only when the FFT window is synchronized with the OFDM symbols. Otherwise intersymbol interference (ISI) will occur. This reduces the usable width of the received signal (the open "eye") at the receiver by a factor of approximately *N*. To extract the usable ISI-free time slot of the received signal, an optical gate must be part of the FFT circuit, such that bandwidth-limited receiver electronics may be used [7].

In OFDM transmission, accumulated group-velocity dispersion (GVD) will introduce crosstalk by shifting the OFDM symbol boundaries in each subchannel, which causes blurring [15,17]. However, since subchannel rates and spacing can be high in our scheme, the sensitivity to GVD is non-negligible. The addition of a cyclic prefix could alleviate the problem, but is difficult to realize within the optical IFFT circuit, as a part of the optical signal would need to be duplicated and delayed increasing the complexity of the scheme.

3.2 OFDM using a frequency comb

At the transmitter, the subchannel rate limitations imposed by electronics may be overcome by using a DWDM-like approach, where the possibility to optically generate precisely tuned

#124508 - $15.00 USD Received 19 Feb 2010; revised 2 Apr 2010; accepted 15 Apr 2010; published 20 Apr 2010

spectral components in frequency space is exploited to directly generate OFDM subcarriers at the correct frequency separation $\Delta\omega$ as required by the OFDM condition (6). A bank of frequency offset-locked laser diodes or an optical comb generator provide subchannel carriers which can be modulated individually [22]. Also the concept of a recirculating frequency shifter (RFS) has been successfully applied to generation of frequency offset-locked subcarriers [23]. A similar approach is used by coherent WDM systems, which forego the OFFT at the receiver in favor of standard optical filters, but require a phase-synchronized transmitter laser bank [24].

In the approach shown in Fig. 8(a), the frequency comb of a pulse source is spectrally separated into subchannel carriers. Each subcarrier, frequency-locked but not phase-synchronized, is then individually modulated and combined to form OFDM symbols. Hence, a corresponding optical FFT receiver can be used to decode the subchannels. The major difference to the IFFT transmitter is that the output corresponding to any one input is not a series of pulses with discrete phases, but a continuous signal with a corresponding optical frequency. This transmitter can be considered as the continuous Fourier transform equivalent of the discrete transform performed by the IFFT.

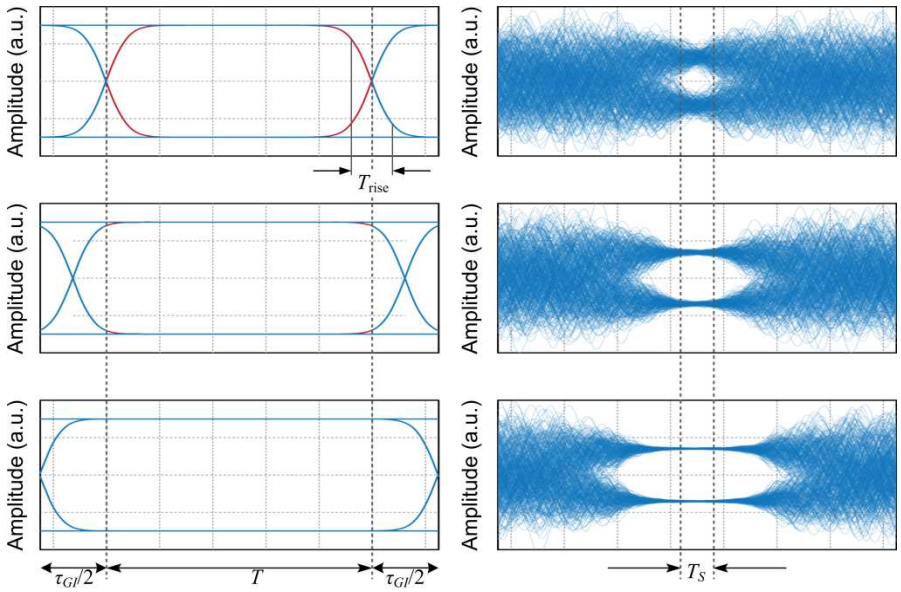

Fig. 9. Function of an OFDM guard interval using the setup of Fig. 8(b) and an 8-FFT. On the left-hand side, the exemplary eye diagram of a single modulated subchannel is shown, as is, on the right side, the received signal before optical gating. If the symbol duration equals the integration interval T, the signal transitions, described by the 10-90% rise/fall time T_{rise} (red), cause inter- and intra-subchannel crosstalk and the received eye is almost fully closed within the observation window of length $T_S = T/N$. With increasing length of the guard interval τ_{GI}, interference vanishes during T. Further increasing the guard interval increases the duration in which the orthogonality condition is fulfilled and thus increases the duration of the open "eye."

In such a transmitter, bandwidth limitations of the modulator will cause subchannel crosstalk because the orthogonality condition (7) cannot be fulfilled in the presence of residual amplitude modulation of the subchannels near the symbol boundaries. The orthogonality condition actually forbids residual modulation of the subcarriers within the FFT window – the phase and amplitude of the complex signal to be encoded must be maintained throughout the symbol time T. This would require the transition from one OFDM symbol to the next to be instantaneous, requiring modulators of infinite bandwidth. Any transition region between adjacent symbols therefore would lead to a violation of the orthogonality condition. If the subchannels are not orthogonal, crosstalk will be generated when performing the FFT in the

#124508 - $15.00 USD Received 19 Feb 2010; revised 2 Apr 2010; accepted 15 Apr 2010; published 20 Apr 2010

receiver. As a result, the portion of the symbol duration usable for detection at the receiver – and thus the width of the gating window is shortened. This is illustrated in Fig. 9(a). Similar to traditional OFDM [16], a remedy is the insertion of a guard interval (corresponding to the cyclic prefix) between symbols so that the *FFT window duration at the receiver will not be changed.* By making the guard interval just long enough to contain the intersymbol transition, the remaining part of the OFDM symbol fulfils the orthogonality condition and receiver crosstalk will only be generated within the guard interval. The width of the open "eye" at the receiver increases, albeit at the cost of a slightly reduced symbol rate. This is illustrated in Figs. 9(b) and 9(c).

An additional increase of the guard interval increases resilience towards accumulated GVD. For an increase of the guard interval length τ_{GI} (beyond that necessary to achieve the required degree of orthogonality) one can keep up with a maximum accumulated GVD B_2,

$$B_2 = \int_{z=0}^{L} \beta_2 \, dz = \frac{\tau_{GI}}{\Delta\omega} \tag{8}$$

where L is the system length, β_2 is the local GVD coefficient and $\Delta\omega$ is the angular bandwidth of the OFDM (super-)channel. By using optical filters to extract a slice of the OFDM channel before performing an FFT of correspondingly lower order, as shown in Fig. 6, the bandwidth $\Delta\omega$ over which GVD may introduce crosstalk is reduced. Thus the resilience towards accumulated GVD increases (see Fig. 10).

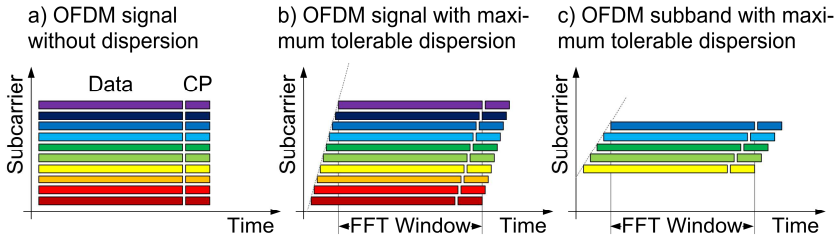

Fig. 10. Mitigating dispersion by means of a cyclic prefix (CP). (a) An OFDM signal with data and cyclic prefix. (b) Frequency dependent delay of subcarriers after transmission due to dispersion. The amount of dispersion that can be tolerated is limited by the length of the cyclic prefix (CP) as all subcarrier symbols must stay within the FFT window. (c) By means of optical filtering, an OFDM subband has been extracted, as discussed in Fig. 6. This way, only the extracted symbols must stay within the FFT window, and thus a larger amount of dispersion can be tolerated.

However, as discussed earlier, it comes at a price. Conventional optical bandpass filters introduce inter-subchannel crosstalk and inter-symbol interference and thus reduce the quality of the received signal. Nevertheless, such a scheme has been successfully used in [24] to extract a single subchannel of an optically generated OFDM signal. The combination of a cascade of DIs and simple optical filters to perform OFDM demultiplexing has also been exploited in the electrical domain. In [23], cascaded delay-and-add elements were used instead of an FFT in order to extract single subchannels out of an optically filtered section of the OFDM channel spectrum. This method reduces cost in terms of time and complexity, but is still limited by the speed of electronics. Another approach to reduce the required electronics speed is multi-band OFDM [25,26], which sacrifices some spectral efficiency for the ability to extract OFDM subbands by tuning the LO laser within the receiver.

#124508 - $15.00 USD Received 19 Feb 2010; revised 2 Apr 2010; accepted 15 Apr 2010; published 20 Apr 2010

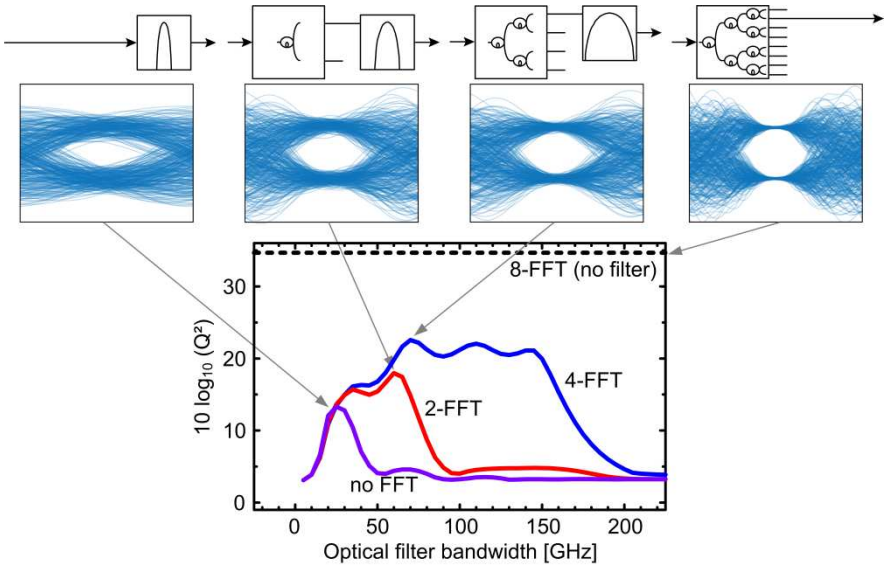

Fig. 11. Achievable quality of the received signal for various FFT filter schemes performed on an 8-channel OFDM signal with 20 GBd on a 25 GHz subcarrier spacings. . The solid red plot shows the signal quality if the FFT is performed with a Gaussian filter as a function of the Gaussian filter bandwidth. The blue and green curves show the signal qualities if one and two DI cascades are used. The black curve shows how a perfect FFT can be performed if the FFT is performed with DIs only.

Exemplary, Fig. 11 shows the dependence of the back-to-back received signal quality, determined in terms of Q,

$$Q = \frac{\bar{I}_0 - \bar{I}_1}{\sigma_0 + \sigma_1} \tag{9}$$

averaged over the in-phase and quadrature components of the central subchannel, versus the bandwidth of a 4th-order Gaussian filter for various simplifying implementations of the optical FFT and for a guard interval of 25% of the OFDM Symbol duration T. In equ. (9), the quantities $\bar{I}$ denote the mean signal values and the symbols σ mean the standard deviations of the received symbol levels (in this case the in-phase and quadrature values of QPSK subchannel signals). The transmitter setup shown in Fig. 8(c) was used with a modulator rise time $T_{\text{rise}} = T/8$ and an optical 200 GHz bandpass filter following the modulator. Clearly, the signal quality deteriorates with the number of DI stages that have been replaced by conventional filters. However, the improvement in residual GVD tolerance may well offset the penalty in systems with a large number of subchannels.

4 Experimental results

To verify the feasibility of the all-optical OFDM generation, including a guard interval, and OFDM demultiplexing by means of the OFFT, we performed a back-to-back experiment which will be briefly described in this section [28].

The OFDM receiver and transmitter is shown in Fig. 12. The transmitter is based on the principles presented in Section 3.2. The frequency-locked subcarriers are generated by a 50 GHz comb generator providing 9 sufficiently strong OFDM subcarriers. The optical comb source is based on two cascaded dual drive Mach-Zehnder modulators that are driven by an electrical clock signal as demonstrated in [24]. These are separated into odd and even channels by a disinterleaver. The odd channels are encoded with PRBS 2^7–1 DPSK data at 28 GBd while the even channels are encoded with 28 GBd DQPSK data, using decorrelated PRBS

#124508 - $15.00 USD Received 19 Feb 2010; revised 2 Apr 2010; accepted 15 Apr 2010; published 20 Apr 2010

2^7-1 sequences for the in-phase and quadrature components. After combination within an optical coupler, the channel spectra overlap significantly and thus can no longer be demultiplexed by standard optical filters. This was verified with the help of simulations and experiments. We end up with a 392 Gbit/s OFDM signal.

The guard interval length was set to 15.7 ps due to the significant rise and fall times of the optical modulator used, and to increase the sampling window size at the receiver. Had we been able to use better performing components, the guard interval could have been reduced significantly without affecting the operation of the optical FFT at the receiver, and thus bring the OFDM symbol rate closer to the subchannel separation frequency $\Delta\omega$.

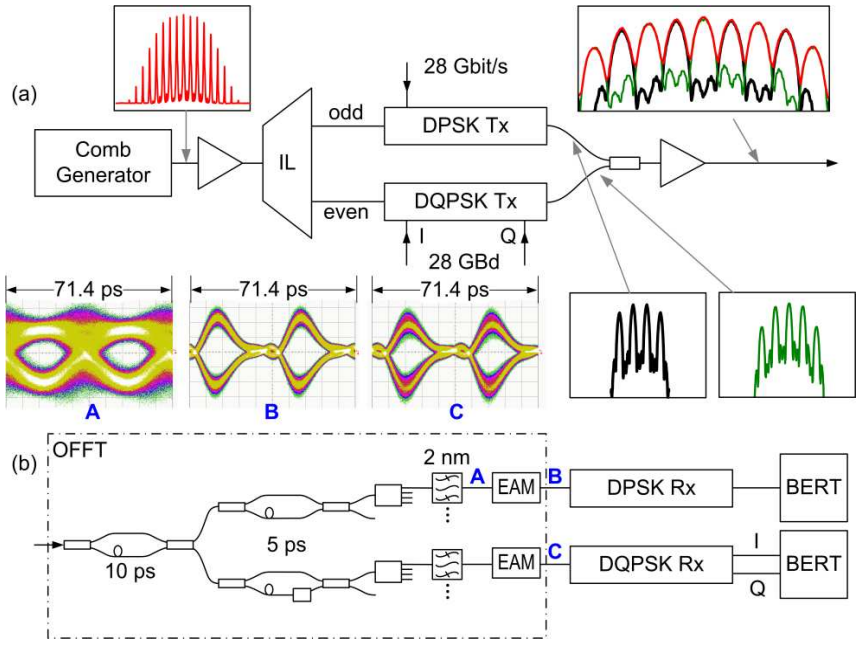

Fig. 12. Setup of OFDM transmission system with (a) transmitter and (b) receiver. Two cascaded Mach-Zehnder modulators generate an optical frequency comb, which is split by a disinterleaver into 4 odd and 5 even channels. Spectrally adjacent subcarriers are modulated alternately using DBPSK or DQPSK modulation. All subcarriers are combined in a coupler and transmitted. The received OFDM signal is processed using the low-complexity OFFT circuit of Section 2.3 with 2 DIs and one standard optical filter. The resulting signals are sampled by electro-absorption modulators (EAM) and detected using DBPSK and DQPSK receivers. Bit error rates were measured with a BERT.The receiver comprises the all-optical FFT scheme followed by a preamplified receiver with differential direct detection. The optical FFT circuit consists of a cascade of two DIs, followed by passive splitters and a bank of bandpass filters. We thus adopt the low-complexity FFT circuit of Section 2.3, partially compensating for the associated performance loss by the increased guard interval. The final element of the OFFT are the EAM sampling gates.

To evaluate the OFFT performance, we compared subcarrier signals after multiplexing/demultiplexing with back-to-back (B2B) signals delivered by the DBPSK and DQPSK transmitters, respectively, in terms of bit error ratio (BER) versus receiver input power.

#124508 - $15.00 USD Received 19 Feb 2010; revised 2 Apr 2010; accepted 15 Apr 2010; published 20 Apr 2010

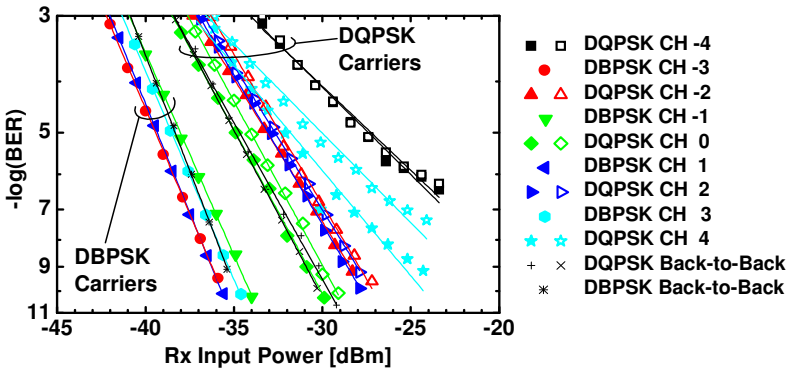

Fig. 13. BER performance of different subcarriers. No penalty is observed compared to back-to-back performance for DBPSK carriers (–3, –1, 1, 3) and no significant penalty for the central DQPSK carriers (–2, 0, 2). A 5 dB penalty or error floor occurs for the two outer DQPSK subcarriers (–4, 4), which are launched with 11 dB less power in the optical comb.

To measure a comparable B2B signal performance, the outputs of the transmitters were gated using the same EAM as it was used in the OFDM receiver. The results depicted in Fig. 13 show no penalty compared to the B2B performance for DBPSK and only a small penalty for the DQPSK channels, owing in part to the large guard interval. The outer channels (labelled "–4" and "4") perform comparatively worse, because these subcarriers are generated with 11 dB less optical power compared to the center channel. The capacity limit for an OFDM channel using this approach is therefore mainly determined by the performance of the frequency comb generator – the number of subcarriers which are generated and the signal-to-noise ratio with which this is done.

5 Conclusion

We have introduced and experimentally demonstrated a practical scheme for optical FFT processing. The implemented OFDM receiver shows no penalty compared to single channel back-to-back performance. As the scheme is not subject to any electronic speed limitations it will allow Tbit/s FFT processing. Also, since the scheme relies on passive optical filters it performs processing with virtually no power consumption and this way may help to overcome the ever increasing energy demand that normally comes with higher speed.

Appendix

Here we show that the DFT / FFT is equivalent to a cascade of DI. We show that the FFT has exactly the frequency response of the DIs.

The DFT in Eq. (1) can be rewritten for continuous input and output signals $x(t)$ and $X_m(t)$

$$X_m(t) = \frac{1}{N} \cdot \sum_{n=0}^{N-1} \exp\left(-\mathrm{j}2\pi n \frac{m}{N}\right) \cdot \delta\left(t - n\frac{T}{N}\right) * x(t) \tag{10}$$

where $\delta(\cdot)$ is the Dirac delta function used to sample the input signal $x(t)$ at N equidistant points within the interval T by means of the convolution operation (*). Due to the numerous convolutions occurring when calculating the impulse response of cascaded elements, it is more appropriate, and equally valid, to do the comparison in the frequency domain. The transfer function $H_m(\omega)$ for the DFT can be obtained by a Fourier transform of (10),

$$\hat{X}_m(\omega) = \underbrace{\frac{1}{N} \cdot \sum_{n=0}^{N-1} \exp\left(-\mathrm{j}2\pi \frac{nm}{N}\right) \exp\left(-\mathrm{j}\omega \frac{nT}{N}\right)}_{H_m(\omega)} \cdot \hat{x}(\omega) \tag{11}$$

#124508 - $15.00 USD Received 19 Feb 2010; revised 2 Apr 2010; accepted 15 Apr 2010; published 20 Apr 2010

In which the caret (^) denotes the Fourier transform. It can be split into two sums corresponding to even and odd n,

$$H_m(\omega) = \frac{1}{N} \cdot \sum_{n=0}^{\frac{N}{2}-1} \left\{ \exp\left(-\mathrm{j}2\pi[2n]\frac{m}{N}\right) \exp\left(-\mathrm{j}\omega[2n]\frac{T}{N}\right) + \exp\left(-\mathrm{j}2\pi[2n+1]\frac{m}{N}\right) \exp\left(-\mathrm{j}\omega[2n+1]\frac{T}{N}\right) \right\} \tag{12}$$

which can be simplified to

$$H_m(\omega) = \underbrace{\frac{2}{N} \cdot \sum_{n=0}^{\frac{N}{2}-1} \exp\left(-\mathrm{j}\frac{2n}{N}[2\pi m + \omega T]\right)}_{\text{FFT of order } N/2} \cdot \underbrace{\frac{1}{2}\left[1 + \exp\left(-\mathrm{j}\left[\omega\frac{T}{N} + \frac{2\pi m}{N}\right]\right)\right]}_{H_{pm,1}(\omega)} \tag{13}$$

Here, $H_{pm,1}$ is the n-independent transfer function for the upper input of a delay interferometer with delay

$$T_p = \frac{T}{N} = \frac{T}{2^p} \tag{14}$$

and additional phase shift

$$\varphi_{pm} = 2\pi\frac{m}{N} - \pi \tag{15}$$

obtained from the cascade of directional couplers and a delay line in the lower arm,

$$\mathbf{H}_{pm}(\omega) = \underbrace{\frac{1}{\sqrt{2}}\begin{pmatrix} 1 & \mathrm{j} \\ \mathrm{j} & 1 \end{pmatrix}}_{\text{output coupler}} \cdot \begin{pmatrix} 1 & 0 \\ 0 & \exp\left[-\mathrm{j}\left(\omega T_p + \varphi_m\right)\right] \end{pmatrix} \cdot \underbrace{\frac{1}{\sqrt{2}}\begin{pmatrix} 1 & \mathrm{j} \\ \mathrm{j} & 1 \end{pmatrix}}_{\text{input coupler}} \underbrace{\begin{pmatrix} 1 & 0 \\ 0 & 0 \end{pmatrix}}_{\substack{\text{upper input} \\ \text{isolation}}} \tag{16}$$

The remainder of expression (13) is the transfer function of the DFT of order $N/2$. Hence, a DFT of order N, with $N = 2^p$, can be implemented optically by cascading a DFT of order $N/2$ and a delay interferometer with delay T/N and output-specific phase shift φ_{pm}. It can be easily verified that the DFT transfer function for $N = 2$ is equal to both outputs of a single DI.

The DI phase φ_{pm} for an upper arm output X_m is the same as that for the lower arm output $\mathrm{j}X_{m+N/2}$. The term describing the $N/2$-order FFT in (13) is also the same for X_m and $\mathrm{j}X_{m+N/2}$ due to its periodicity. Thus both outputs of a single DI can be used to obtain different coefficients of the DFT, resulting directly in the optical FFT scheme of Fig. 3.

Acknowledgments

David Hillerkuss and Jingshi Li acknowledge financial support from the Karlsruhe School of Optics & Photonics (KSOP) and the German Research Foundation (DFG). We also acknowledge partial support by the European Network of Excellence EURO-FOS.

#124508 - $15.00 USD Received 19 Feb 2010; revised 2 Apr 2010; accepted 15 Apr 2010; published 20 Apr 2010